Non-data Aided Rician Parameters Estimation with Redundant GMM for Adaptive Modulation in Industrial Fading Channel

Guobao Lu, *Student Member, IEEE,* Xuewu Dai, *Member, IEEE,* Wuxiong Zhang, *Member, IEEE,* Yang Yang, *Fellow, IEEE,* and Fei Qin, *Member, IEEE*

***Abstract*—Wireless networks have been widely utilized in industries, where wireless links are challenged by the severe non-stationary Rician fading channel, which requires online link quality estimation to support high quality wireless services. However, most traditional Rician estimation approaches are designed for channel measurements and work only with non-modulated symbols. Then, the online Rician estimation usually requires *a priori* aiding pilots or known modulation order to cancel the modulation interference. This paper proposes a non-data aided method with redundant Gaussian mixture model(GMM). The convergence paradigm of GMM with redundant sub-components has been analyzed, guided by which, the redundant sub-components can be iteratively discriminated to approach the global optimization. By further adopting the constellation constraint, the probability to identify the redundant sub-component is significantly increased. As a result, accurate estimation of the Rician parameters can be achieved without additional overhead. Experiments illustrate not only the feasibility but also the near optimal accuracy.**

***Index Terms*—Rician Parameters, Maximum Likelihood Estimation, Non-data Aided, Gaussian Mixture Model, Convergence**

I. Introduction

THE wireless channel of fixed wireless link in industrial scenario has been investigated over decades [1]–[8], where the massive metal surfaces lead to complex fading channels due to the severe multi-path effect. In a fixed wireless link, at least one Line of Sight(LoS) path exists to guarantee the reliability, while all other non-LoS multiple paths vary according to different spatial locations. The combination effects of these homological paths are usually static over time in typical indoor environments, but will be dynamic in industrial environments. This is due to the fact that the moving objects near wireless links will generate dynamic paths and perturb the stationary scattered paths. As a result, both the specular and scattered power of received signals will be time-varying with specific pattern rooted in the arbitrary mobility pattern of moving objects [7]. Such effects have been observed and termed as the non-stationary temporal fading [2]–[7], where the envelope of received signals from the temporal fading channel usually follows the Rician distribution with time varying nature. In such fading channel, the internal thermal noise won't be the only source of transmission error, as the scattered power will also deviate I/Q symbols from expected constellations. Considering the time varying nature of the temporal fading channel, these Rician parameters must be updated on-line to obtain an not only accurate but also realtime link quality metric. Otherwise, the transceiver may take wrong actions due to the inaccurate link quality information, resulting degraded performances in both transmission and application layers [9], [10]. On the other side, accurate Rician parameters can significantly increase the link quality estimation performance in the non-stationary industrial fading channel [7].

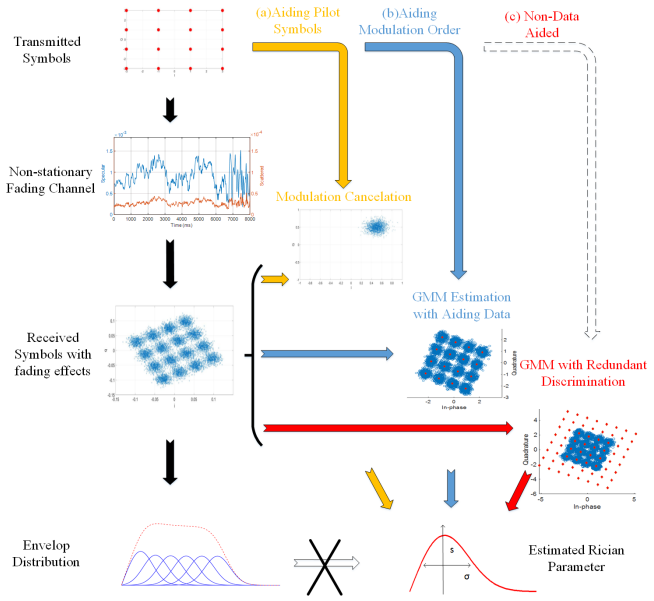

Fig. 1. The scheme of utilizing redundant sub-components based GMM for non-data aided Rician parameter estimation in a temporal fading channel.(best view in color)

The estimation of Rician parameters is of considerable interest. The early approaches are usually designed for the measurement of static or stationary fading channel in an offline pattern, i.e., the I/Q symbols are unique and utilized only for the channel measurement. Nonetheless, these algorithms cannot support online channel estimation, since the existence of modulated symbols will interfere the estimation by discretizing the received symbols into clusters in the constellations, as

This work was supported in part by the Nature Science Foundation of China under Grant 62071450, in part by Heilongjiang Provincial Key Science and Technology Project under Grant 2020ZX03A02, in part by the Scientific Instrument Developing Project of the Chinese Academy of Sciences under Grant YJKYYQ20170074, in part by the Fundamental Research Funds for the Central Universities, and in part by the National Key Research and Development Program of China under Grant 2019YFB2101602 and Grant 2020YFB2104300.

illustrated by the black arrows in Fig.1. As a result, the classical moment based and phase based Rician estimation methods cannot be directly applied, and have to work with pilot symbols or preambles to cancel the self-interference caused by modulated signals [11], [12], shown in Fig.1 with the orange arrows. This method has been widely utilized and named as data aided mode or pilot aided mode. Without any doubt, the data-aided mode fails to utilize massive modulated I/Q samples to achieve higher accuracy, while decreases the efficiency of bandwidth due to increased overhead.

In recent years, many efforts have been focused on the non-data aided Rician parameters estimation [11], [13], [14]. A state of the art work in [15] employs the Gaussian Mixture Model (GMM) to design a more general framework for the Rician parameter estimation with modulation interference. In detial, all the received I/Q symbols are fitted into a mixture of two dimensional Gaussian distributions (termed as *sub-component* in this paper, also known as *Gaussian kernel*). This method can fully utilize the modulated I/Q symbols to approach the optimized performance, but only works under the condition that the information of modulation order in the received packets is known *a priori*. This condition is necessary to enable the appropriate convergence of Expectation-Maximization (EM) algorithm for GMM. This approach is illustrated by the blue arrows annotated with 'Aiding Modulation Order' in Fig.1. As expected, the time varying temporal fading channel will trigger frequent adaptations in modulation order to approach the Shannon limit, which requires frequent exchanges of modulation order to satisfy this assumption.

In order to address the challenges caused by the frequently changed modulation order in the harsh industrial environment, this paper aims to develop a novel adaptive Rician channel parameter estimation method without the requirement of *a priori* information on the modulation order. Intuitively, the classical EM algorithm for GMM fitting process will be best converged only when the preset number of sub-components matching the number of sample clusters, i.e., the modulation order. Without this information, although the envelope may still have the possibility to fit the ground truth, the distribution of each sub-components will be biased and cannot be utilized for Rician parameter estimation. As shown in Fig.1 with red arrows, it is straightforward to make a hypothesis that the GMM can be initialized with more than necessary sub-components, which will be recognized and removed in the convergent process to approach the global optimization. To achieve this aim, this paper first analyzes and formalizes the convergence pattern of GMM with redundant sub-components. This paradigm has been utilized to discriminate the redundant sub-components iteratively, which can be further strengthened with constellation constraints. Such constraints will form a binary classification problem with significantly increased discrimination capability, convergence rate and the converged accuracy. Then the proposed method features not only high accuracy but also affordable implementations cost for most wireless platforms.

The contribution of this paper can be summarized in three folds:

- We, for the first time, reveal the convergence patterns of GMM with redundant sub-components, which have been formalized with a theoretical framework.
- We integrate the constellation constraints and the convergence paradigm of redundant GMM to essentially increase the discrimination capability for redundant sub-components.
- We design a generalized non-data aided method to estimate Rician parameters with extremely high performance and affordable cost for non-stationary temporal fading channel in industrial networks.

The rest of this paper is outlined as follows: section II provides related works while section III discusses the problem formulation. The paradigm of redundant components based GMM is presented in section IV, while the constrained convergence with constellations is provided in section V. Experiments results from numerical simulations and industrial sites are utilized to validate the proposed algorithm in section VI, followed by the conclusion in section VII.

II. Related Works

The investigations on the fading channel in industrial scenarios last over decades. The early work in [1], [2] focus on the measurement-based approaches, the results of which validate the effectiveness of the classical propagation principle and also propose the existence of heavy temporal fading effects. The work in [3] examines the more general indoor propagation channel and suggests that the channel performance varies in different scenarios. A state of the art survey on the industrial fading channel has been provided in [5], which confirms the temporal fading effects and concludes that in-depth investigations on this topic are still needed.

Similarly, the estimation of the Rician K factor has been studied over decades as well. The early approaches work with the envelope of received signals and rely on the moment-based estimation method, which suffers from the computational efficiency and accuracy problems. In [16], K was estimated by equating a function of K to a ratio of the measured first and second-order moments of the envelope. Another closed-form estimator for K is derived based on the second and fourth-order moments of the envelope [12], [17], [18]. Instead of the moment based approaches, some work [19]–[21] choose to further utilize the phase information from I/Q symbols in the wireless communication through the Maximum Likelihood Estimation (MLE) or Maximum *a posteriori* (MAP) method to increase the reliability and accuracy.

However, all the above estimators are usually designed for channel measurement of static or stationary fading channel, i.e., the I/Q stream are utilized only for channel measurement system. Nonetheless, these algorithms can not be simply applied into online Rician estimation system with time varying temporal fading channel. Then, these algorithms have to work with extra pilot symbols to cancel the self-interference from modulation [11], [12], [18]. These data-aided methods not only fail to utilize the huge amount of modulated I/Q samples to improve the estimation accuracy, but also reduce the throughput of wireless link with the overhead caused by the additional pilot symbols.

To improve the estimation accuracy and bandwidth efficiency, many efforts have been made to waive the aiding data in Rician parameter estimation. The Auto-Correlation Function (ACF) was adopted in [11] to avoid the data aided requirement, but it cannot be applied to M-ary Phase Shift Keying (M-PSK) due to the null ACF. The fourth-order cross moment statistic has been utilized in [13], [14] to avoid the aiding data, which can only work in the specified Single Input Multiple Output (SIMO) scenarios, i.e., not applicable in other common scenarios, especially the industrial scenario. In [15], an estimator of Rician factor is derived with constellation constrained GMM method, which waives the requirement of aiding pilot symbols but still needs prior information of modulation order. Similarly in [22], the GMM has been employed to characterize the temporal fading channel as well, but utilizes the inter-frame information to decrease the iteration cost.

Recently, adaptive clustering attracts research interests [23], [24]. The work in [23] follows the similar principle of this paper, which assumes a large number sub-components at the initial stage and recognizes the redundancy through message exchanges among samples. As expected, the computation efficiency will be a challenge, while this work proposes a global statistics to recognize the redundancy. The work in [24] provides a guidance to choose the optimized cluster centers. However, both work are the data driven methods and rely on the distance between samples, thus fail to utilize the *a priori* knowledge of Gaussian distribution in Rician estimation.

III. Problem Formulation

In most industrial deployments, the transmitted signals will be reflected, scattered, or diffused with the surrounding massive metal surfaces. Consequently, part of these additional signals along with the original LoS signal arrive at the receiving antenna with different propagation delays τ, amplitude attenuation C, and the phase shifts ϕ. The received combination of these homological signals will be varying over time and distance, which is termed as the multipath fading. Among numerous fading channels, the Rician fading with at least one strong LoS path is most common in industrial environment and can be modeled by [25]:

$$\begin{aligned} h(t) &= C_0 e^{j\varphi_0}\delta(\tau-\tau_0) + \sum_{n=1}^{N} C_n e^{j\varphi_n}\delta(\tau-\tau_n) \\ &= \sqrt{\frac{K\Omega}{K+1}}h_{sp}(t) + \sqrt{\frac{\Omega}{K+1}}h_{sc}(t), \end{aligned} \tag{1}$$

where $h_{sp}(t)$ is termed as specular component contributed by LOS path or other strong dynamic path, while $h_{sc}(t)$ is termed as scattered component representing all other scattered paths. Ω represents the average power of the received signal, while K represents the ratio between specular power s^2 and scattered power $2\sigma^2$.

The received signal $R(t)$ will be mainly contributed by the convolution between the transmitted signal $S(t)$ and the impulse response $h(t)$:

$$R(t) = S(t) * h(t) + \omega(t), \tag{2}$$

where $\omega(t)$ is the internal thermal noise inside the receiver system. As shown in eq.(2), the channel fading $h(t)$ and noise $\omega(t)$ will degrade the quality of received symbols in a different way. The first one is by convolution and the later one is additive, but their resulting impacts on $R(t)$ are the same in the sense of deviating the received signal from its expected ideal constellation. In particular, the scattered power of the Rician fading channel has a similar effect as white noise in the industrial temporal fading channel. Consider the fact that the specular power compared with the scatter power(i.e., the Rician parameter K) usually is much larger than the ratio between specular power and internal thermal noise(i.e., the SNR). It is widely accepted that the link quality of multipath fading channel can be represented better by the Rician parameter K, than by the received signal strength or its variations. This is particularly true in the industrial environment where heavy fading is not unusual.

In this context, the envelope of received signals $R(t)$ after Rician fading channel will follow the Rician distribution [25]:

$$f_R(r_n|s,\sigma) = \frac{r_n}{\sigma^2}\exp\left(-\frac{r_n^2+s^2}{2\sigma^2}\right)I_0\left(\frac{s\cdot r_n}{\sigma^2}\right), \tag{3}$$

where r_n is the envelope of the n^{th} sample. Since s and σ represent the direct observation of the fading channel, it is reasonable to utilize Rician parameters as accurate link quality estimations, especially the K factor. These parameters can also be reflected in the fading signal received by the receiving end. Nonetheless, it should be award that the internal thermal noise $\omega(t)$ will also applied on the σ and cause estimation error. Due to the existence of a zero order Bessel function $I_0(\cdot)$, the estimations of Rician parameters usually rely on the iterative based moment statistics, which require large number of samples and may suffer from the loss of accuracy and reliability [26], [27].

To overcome this limitation, the phase information in the received I/Q symbols has been further utilized to obtain a reliable closed form solution. The joint Power Density Function (PDF) with both the envelope and phase can be derived from eq.(3):

$$\begin{aligned} &f_{R,\Phi}(r_n,\phi_n|s,\sigma,\phi_0) = \\ &\frac{r_n}{2\pi\sigma^2}\exp\left(-\frac{r_n^2+s^2-2r_n s\cos(\phi_n-\phi_0)}{2\sigma^2}\right), \end{aligned} \tag{4}$$

where ϕ_n is the introduced phase of received I/Q symbols, ϕ_0 is the phase variation caused by the specular components in the fading channel. Now, a closed form solution can be simply obtained following the classical Maximum Likelihood Estimation(MLE) method, which increases not only the estimation accuracy but also the calculation efficiency [21].

However, the above estimation methods are proposed for the channel measurement, which means the transmitted symbols are unique, i.e., without modulated information. As shown in Fig.1, once the modulation was involved, the transmitted symbols will be distributed over constellations with various amplitudes and phases, which will introduce unknown modulation parameters in the transmitted signal $S(t)$, i.e., $a_m \in \boldsymbol{A}$ and $\phi_m \in \boldsymbol{\Phi}$, into eq.(4). As a result, the closed form solution will no longer work. A widely utilized method to against this

problem is the employment of pilot symbols or preambles, i.e., a limited number of symbols with *a priori* modulated information, which can be used to cancel the modulation effect in the receiver side. As expected, this method not only suffers from low accuracy due to the limited number of pilot symbols, but also wastes the bandwidth by the occupation of pilots.

On the other side, the received I/Q symbols corresponding to each constellation point will form a two-dimensional Gaussian distribution under the assumption of independent identical distribution sampling over Rician fading model. Then, all the received symbols will consist several clusters, and can be modeled as two-dimensional Gaussian PDFs (Probability Density Functions). The constitution of these Gaussian PDFs can be further modeled as a Gaussian Mixture Model (GMM). Through the reverse of the Jacobian determinant, eq.(4) can be expressed with a two dimension Gaussian distribution:

$$G(x_{i,n}, x_{q,n}|\mu_i, \mu_q, \sigma_i, \sigma_q) = \frac{1}{\sqrt{2\pi\sigma_i^2}} exp(-\frac{(x_{i,n}-\mu_i)^2}{2\sigma_i^2}) \frac{1}{\sqrt{2\pi\sigma_q^2}} exp(-\frac{(x_{q,n}-\mu_q)^2}{2\sigma_q^2}), \tag{5}$$

where μ_i and μ_q are contributed by the specular paths, σ_i and σ_q are contributed by all the scattered paths, respectively. Then, the GMM can be formulated as:

$$p(\boldsymbol{x_n}; \boldsymbol{\theta}) = \sum_{m=1}^{M} \omega_m G(\boldsymbol{x_n}|\boldsymbol{\theta_m}), \tag{6}$$

where $\boldsymbol{x_n}$ the brief of the complex baseband symbols; $\boldsymbol{\theta_m}$ is the brief of Gaussian parameters; $\boldsymbol{M}$ is the modulation order, e.g. 4 for QPSK, 8 for 8-PSK and 16 for 16QAM. This can be intuitively understand as a mixture with M Gaussian sub-components, while ω_m is the weight of each sub-component.

Under this context, the log-likelihood function of eq.(6) can be obtained:

$$L = ln(P(\boldsymbol{X}|\boldsymbol{\theta})) = \sum_{n=1}^{N} ln(\sum_{m=1}^{M} \omega_m G(\boldsymbol{x_n}|\boldsymbol{\theta_m})). \tag{7}$$

Due to the existence of logarithm over sum, this equation failed to be analytically solved. By applying the Jensen inequality, the lower bound of above equation can be obtained:

$$Q = \sum_{n=1}^{N} \sum_{m=1}^{M} p_{n,m} ln(\frac{\omega_m G(\boldsymbol{x_n}|\boldsymbol{\theta_m})}{p_{n,m}}), \tag{8}$$

where $p_{n,m} = \frac{\omega_m G(x_n|\theta_m)}{\sum_{m=1}^{M} \omega_m G(x_n|\theta_m)}$ represents the probability that the n^{th} symbol belongs to the m^{th} sub-components,which was evaluated by applying the n^{th} symbol, i.e., x_n into each sub-component comparing with the integrated GMM PDF. The classical Expectation-Maximization (EM) algorithm will try to maximize Q through MLE in M step, and calculate Q with updated estimate $\boldsymbol{\theta}$ in E step, the iterative repeat of which will lead to the convergence of global optimal. If recall eq.(5), the converged $\boldsymbol{\theta}$ will be the equalized form of Rician parameters, which only requires simple linear transformation.

Without any doubts, the convergence of EM algorithm is costly, especially with high modulation order, which prevents its practical application. In fact, when the modulation order M is large, the EM algorithm will usually fail to approach the optimal, i.e., the ground truth of the solution. For example, in 16QAM, the Degree of Freedom (DoF) or known as the dimension of solution space will be $7 \times 16 = 102$. The authors in [15] propose an efficient method to significantly accelerate the convergence of EM algorithm by transforming the optimal search into lower dimension solution space, which essentially enables the implementation of GMM based method. Although this work removes the requirement of aiding symbols like pilot symbols or preamble, it still relies on the *a priori* information of modulation order to guarantee the convergence of EM algorithm, i.e., M, which can only be exchanged through specific packets. Hinted by recent progress in adaptive clustering [23], [24], we are motivated to make essential investigation of the EM based GMM estimation and remove this residual *a priori* requirements.

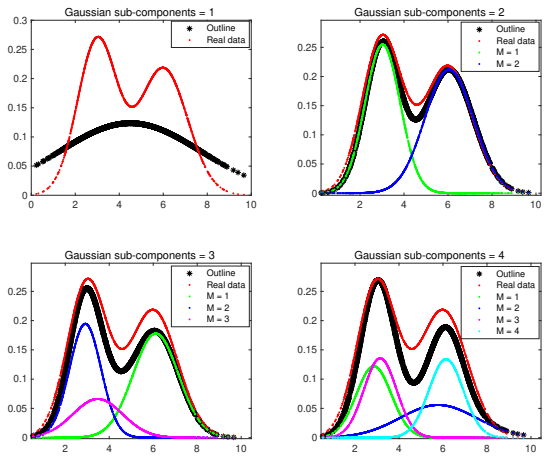

Fig. 2. The fitting results of Gaussian mixture model with different numbers of sub-components in a two clusters scenario, i.e., $M^0 = 2, M = 1, 2, 3, 4$

IV. The Convergence Paradigm with Redundant Sub-Components Based GMM

As discussed in section II, the motivation of this paper is to find an efficient method to guarantee the convergence of EM algorithm without *a priori* modulation order, i.e., the cluster numbers in the constellation. It is straightforward to initialize GMM with redundant number of sub-components, following by the discrimination and deletion of redundant sub-components until the ground truth. Clearly, the essential challenge is how to distinguish the redundant sub-components, which, to the best of authors' knowledge, has never been investigated before.

In Fig.2, a simple but descriptive example has been provided, where two one-dimension clusters following Gaussian distribution [1] have been employed to generate sample data. For easy discussion, M^0 has been defined as the ground truth of cluster numbers. These samples will be processed by

[1]One-dimension data was employed due to the better visualization effect, similar effects exist in all dimensions

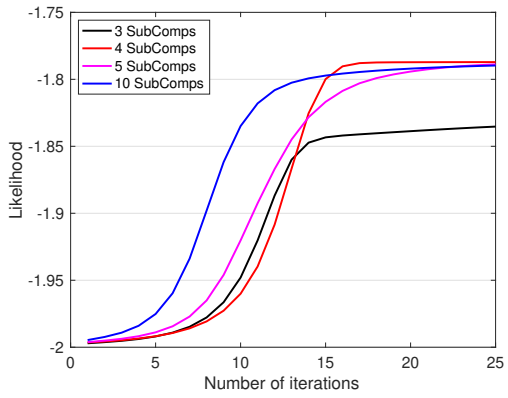

Fig. 3. The convergence progress of Likelihood with different number of sub-components, $m^0 = 4$ (best view in color)

classical EM algorithm with different number of preset sub-components, i.e., $M = 1, 2, 3, 4$. The results have been shown in four sub-figures, respectively. The ground truth has been shown with red dots, while the envelope of final fitted GMM has been shown with black dots. The fitted sub-components have been shown with various colors. Easy to notice that the fitting error is only significant in the scenario with $M = 1$, i.e., less than the ground truth. This is reasonable that one Gaussian distribution can never fit two Gaussian distributions. In all other scenarios with $M \geq 2$, the converged envelops have shown satisfied fit goodness. This explains why the discrimination of redundant sub-components has been ignored before: the EM algorithm doesn't need to delete the redundant sub-components to approach a good fitted envelope.

However, the fit goodness of envelope is not enough for the application of Rician parameters estimation. This is due to the fact that the estimation of Rician parameter is rely on the fit goodness of sub-component not the overall envelop, i.e., s is linearly calculated from all $\boldsymbol{\mu_m}$, while σ is linearly calculated from all $\boldsymbol{\Sigma_m}$. With redundant sub-components shown in Fig.2, there will be variation on each sub-components, which will result in the significant estimation error of Rician parameters.

To better characterize this effect, the convergence progresses over time domain have been provided in Fig.3, where the same findings can be concluded, i.e., the likelihood will finally approach the global optimal with $M \geq M^0$. Without any doubts, when the number of sub-components in GMM is equal to the number of clusters, i.e., $M = M^0$, the likelihood value can best approach the global maximum. The term of 'best' refers both the value and the convergence rate. Based on these observations, the following Lemma can be formalized:

Lemma 1. *Given the maximum likelihood Q can be obtained in the EM estimation of GMM, s.t. $M = M^0$. Then, if $M > M^0$, the maximum likelihood Q_{M^0} can still be approached:*

$$\lim_{i \to +\infty} Q_M \to max(Q_{M^0}), \tag{9}$$

where i is the iteration index.

Proof. First consider the scenario with $M^0 = 1$ and $M = 2$, let $\Delta m = M - M^0 = 1$.

Obviously, a solution can be found with $\boldsymbol{\mu_1} = \boldsymbol{\mu_2} = \boldsymbol{\mu}$, $\boldsymbol{\Sigma_1} = \boldsymbol{\Sigma_2} = \boldsymbol{\Sigma}$, and $\omega_1 = \omega_2 = 1/2$, which satisfies

$$\begin{aligned} &\sum_{n=1}^{N} \sum_{m=1}^{M^0} p_{n,m} ln(\frac{\omega_m G(\boldsymbol{x_n}|\boldsymbol{\theta_m})}{p_{n,m}}) \\ =&\sum_{n=1}^{N} \sum_{m=1}^{M^0+\Delta m} p_{n,m} ln(\frac{\omega_m G(\boldsymbol{x_n}|\boldsymbol{\theta_m})}{p_{n,m}}). \end{aligned} \tag{10}$$

Without loss of generality, for any $\Delta m \in \mathbb{N}_+$, at least one solution with $\forall \boldsymbol{\mu_m} = \boldsymbol{\mu}$, $\forall \boldsymbol{\Sigma_m} = \boldsymbol{\Sigma}$, and $\forall \omega_m = 1/M$ can satisfy eq.(10).

For the scenarios with $M^0 > 1$, we can let the first $M^0 - 1$ clusters be fitted with the same sub-components, and let the last cluster be fitted with Δm sub-components. Repeating the above derivation, at least one solution can be found which can still satisfy eq.(10). □

Lemma 2. *If $M < M^0$, the approachable likelihood Q_M will be less than the maximum likelihood Q_{M^0}.*

Proof. If $\Delta m = M^0$, $M = 0$. The likelihood Q_M will be 0, which will be definitely less than $max(Q_{M^0})$.

In the scenario with $M^0 = 1$, the only possible $\Delta m = 1 = M^0$, which is equal to the above derivation.

In the scenario with $M^0 = 2$ and $\Delta m = 1$, if eq.(10) can be satisfied, then the following equalized derivation should hold:

$$\begin{aligned} &KLD[p_1(\boldsymbol{x_n}|\boldsymbol{\theta_1})||p_2(\boldsymbol{x_n}|\boldsymbol{\theta_2})] \\ =&\int G(\boldsymbol{x_n}|\boldsymbol{\theta_1}) ln \frac{G(\boldsymbol{x_n}|\boldsymbol{\theta_1})}{\sum_{m=1}^{2} \omega_m G(\boldsymbol{x_n}|\boldsymbol{\theta_m})} dx = 0, \end{aligned} \tag{11}$$

where KLD refers to the Kullback-Leibler Divergence. eq.(11) can be intuitively understand as: $\exists \theta_1$ makes a single Gaussian distribution perfectly fitting a GMM consisted by two sub-Gaussian distribution, which is obviously an antinomy.

Without loss of generality, for any $\Delta m \in \mathbb{N}_+$ and $M^0 > 2$, we can let the first $M^0 - \Delta m$ clusters be fitted with the same sub-components, and let the last ΔM clusters be fitted with a single Gaussian PDF. Similar as the above derivation, easy to conclude that no solution can be found to satisfy eq.(10), yet Q_M will be less than $max(Q_{M^0})$ □

With simple derivation, we can obtain the following corollaries, which can be utilized to guide the algorithm design.

Corollary 1. *By deleting $\Delta m \leq M - M^0$ sub-components, the re-converged likelihood Q' will be no less than the likelihood Q before deletion.*

Proof. If $\Delta m \leq M - M^0$, then the new $M' \geq M^0$. By applying Lemma 2, $Q' \to max(Q_{M^0})$, while $Q \to max(Q_{M^0})$. Then $Q' \to Q$. □

Corollary 2. *By deleting $\Delta m > M - M^0$ sub-components, the re-converged likelihood Q' will be less than the likelihood Q before deletion.*

Proof. If $\Delta m < M - M^0$, then the new $M' < M^0$. By applying Lemma 3, $Q' < max(Q_{M^0})$, while $Q \to max(Q_{M^0})$. Then $Q' < Q$. □

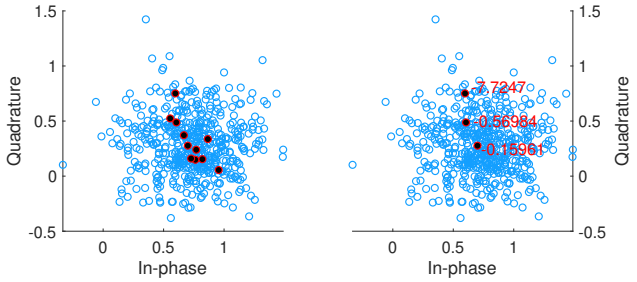

Fig. 4. The likelihoods of sub-components versus the converged locations.

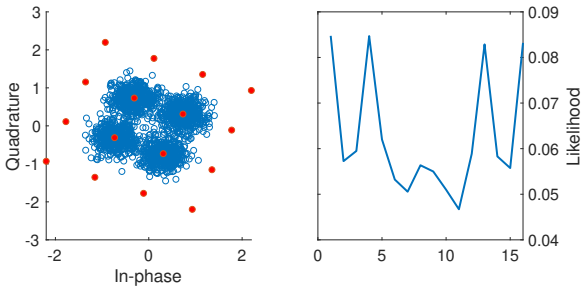

Fig. 5. The binary classification with constellation topology constraints

With Corollary 1 and Corollary 2, the algorithm can identify when the final convergence has been met, i.e., $M = M^0$. The next problem is to find the right sub-components to delete. As shown in Fig.4, when the GMM with redundant sub-components converges, the sub-components located in different positions vary with different likelihoods l_m:

$$l_m \approx q_m = \sum_{n=1}^{N} p_{n,m} ln(\frac{\omega_m G(\boldsymbol{x_n}|\boldsymbol{\theta_m})}{p_{n,m}}). \tag{12}$$

The sub-components located in the data-intensive area are named as near-end components, and the sub-components located in the sparse data position are named far-end components. Intuitively, the algorithm will tend to delete far-end components to enable fast convergence in the next iteration. As the likelihoods of near-end components will usually be large than far-end components, we can utilize soft-max function to classify the sub-components as near-end components and far-end component according to their likelihoods.

$$softmax(l_m) = \frac{\exp(l_m)}{\sum_{m=1}^{M} \exp(l_m)}. \tag{13}$$

In each iteration cycle, the far-end components will be deleted, and the rest will be reorganized as a new Gaussian mixture model for the next convergence. As this is essentially a semi-blind deletion, such iteration will be ended until Corollary 2 satisfied, which hints that more than necessary sub-components have been deleted in the last iteration. With aid from a simple buffer, the algorithm can reverse back to the last iteration. However, as the algorithm still don't know the correct number to delete, we can simply delete one sub-component in each iteration to instead. The overall iteration will be terminated by Corollary 1 satisfied in the current iteration cycle while Corollary 2 satisfied in the last iteration.

V. The Convergence Acceleration with Constraint of Constellation Topology

In section III, we propose the convergence paradigm of GMM with redundant sub-components, which, in the first time, can converge to the exact modulated clusters without any *a priori* information. In this section, we will introduce constellation topology constraints to the proposed algorithm, which will significantly increase the convergence speed by forcing sub-components to form a binary classification pattern in the likelihood space, i.e., the algorithm can now simply identify the correct redundant sub-components.

Considering a transceiver pair over fading channel, the topology of transmitted constellations will be constant in each packet. The fading channel will only cause all the constellations, as an indivisible whole, to scale in attenuation s, to rotate in angle ϕ_0, and to scatter with the variation of σ in amplitude. This is due to the fact that the relative distances and angles among constellations are constrained due to modulation scheme. Therefore, we can use a complete set of constellation topology, which contains all the potential constellation diagrams in an application, to spatially constrain the redundant sub-components of the GMM.

With some algebra, the PDF of GMM can be converted to polar coordinates, and involve topology constraints as:

$$\begin{aligned} f_{R,\Phi}(r_n, \phi_n|s, \sigma, \phi_0) &= \sum_{m=1}^{M} \frac{r_n}{2M\pi\sigma^2} \\ \exp(-&\frac{r_n^2 + a_m s^2 - 2a_m r_n s\cos(\phi_n - \phi_0 - \phi_m)}{2\sigma^2}), \end{aligned} \tag{14}$$

where $r_n^2 = r_{i,n}^2 + r_{q,n}^2$ represent the envelope of received signal, $\phi_n = actan(r_{i,n}/r_{q,n})$ is the offset angle of each sampling point. $a_m \in \boldsymbol{A}$ and $\phi_m \in \boldsymbol{\Phi}$ is the ideal locations of the m^{th} cluster, which are the *a priori* information provided by the complete set of constellation schemes. It is easy to notice that eq.(14) will regulate the gradient search only in s, σ and ϕ_0. Following similar derivations, the pseudo-MLE of parameters in the Maximization step can be easily obtained.

With eq.(14), the convergence will force the likelihoods of sub-components to show a clear binary classification pattern. As shown in Fig.5, only part of sub-components can approach the data cluster, while the rest will be regulated away with topology space $\boldsymbol{A}$ and $\boldsymbol{\Phi}$. This can be formalized as:

Lemma 3. *With constellation topology constraint, the converged likelihood of each sub-components will form a binary classification pattern.*

Proof. After convergence, the likelihood function can be rewrite as:

$$Q = \sum_{f \in F} L_f + \sum_{e \in E} L_e \tag{15}$$

where $L_f = \sum_{n=1}^{N} p_{n,f} ln(\frac{\omega_f G(\boldsymbol{x_n}|\boldsymbol{\theta_f})}{p_{n,f}})$ refers the far-end components, $L_e = \sum_{n=1}^{N} p_{n,e} ln(\frac{\omega_e G(\boldsymbol{x_n}|\boldsymbol{\theta_e})}{p_{n,e}})$ refers the near-end components.

For $\forall e \in E$, the sub-components have already approached the clusters, i.e., $\boldsymbol{\mu}'_{\boldsymbol{e}} \to \boldsymbol{\mu}_{\boldsymbol{e}}$, $\boldsymbol{\Sigma}'_{\boldsymbol{e}} \to \boldsymbol{\Sigma}_{\boldsymbol{e}}$. L_e can be approximated as:

$$L'_e \approx \sum_{n \in e} p_{n,e} ln \frac{\omega_e G(\boldsymbol{x_n}|\boldsymbol{\theta_e})}{p_{n,e}} + \sum_{n \notin e} 0 \cdot ln \frac{\omega_e G(\boldsymbol{x_n}|\boldsymbol{\theta_e})}{p_{n,e}} \quad (16)$$

That is, the likelihood will be mainly contributed by the approached clusters e, while the all other data samples will contribute close to 0.

For $\forall f \in F$, due to the topology constraint, the sub-component is away from any clusters. As a result, all $p_{n,f}$ will approximate zero, i.e., $L'_f \to 0$.

Then $\forall L_e > \forall L_f$, Lemma proofed. □

As shown in Fig.5, Lemma 3 regulates the sub-components to form a binary classification. Then, the proposed method can simply and accurately distinguish redundant sub-components, which essentially reduces the complexity of proposed method, i.e., only one additional deletion process. As shown later in the experiment section, the iterative cycles can be significantly reduced, which enables the wide application of proposed method. The final algorithm has been provided below.

Algorithm 1 Constrained Redundant GMM Method

Require: complete set of constellations $\boldsymbol{A}$ and $\boldsymbol{\Phi}$, converge threshold Th,received I/Q symbols $r_{i,n}, r_{q,n}$
Ensure: $i = 1, I = 1, l_0 = 0, L_0 = 0$
  while $L_I - L_{I-1} > Th$ **do**
    while $l_i - l_{i-1} > Th$ **do**
      Calculate $\boldsymbol{P}$ in E step
      Calculate s, σ, ϕ_0 in M steps
      $l_{i,m} \leftarrow likelihood, q_m$
      $l_i \leftarrow \sum l_{i,m}$
      $i \leftarrow i + 1$
    end while
    delete sub-components with $l_m < mean(l_m)$
    $L_I \leftarrow l_i$
    $I \leftarrow I + 1$
  end while
  return s, σ

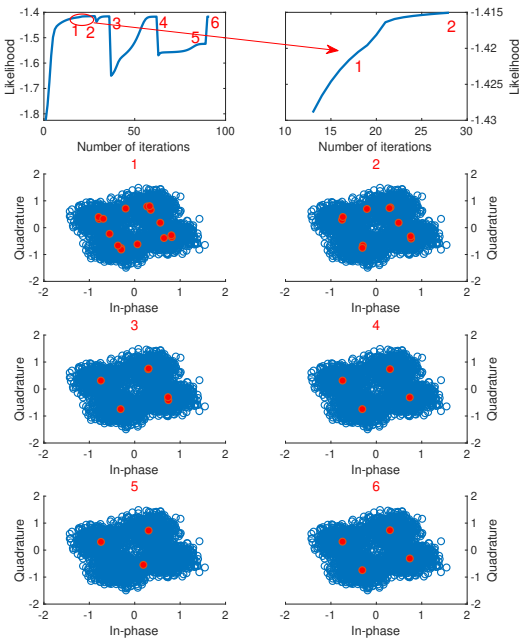

Fig. 6. The converge process with proposed R-GMM (best view in color).

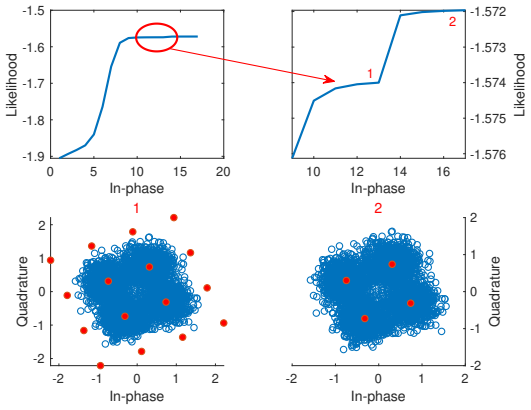

Fig. 7. The converge process with proposed CR-GMM (best view in color).

VI. Experiment Results

A. The convergence of proposed algorithms

The intuitive results of how the proposed two methods performing will be provided first in Fig.6 and Fig.7. The converge process shown in Fig.6 is based on the redundant sub-components based GMM estimation method discussed in section III, which will be named as Redundant GMM (R-GMM) in the following discussion. While the same time, The converge process shown in Fig.7 is based on the constellation topology constrained estimation method discussed in section IV, which will be named as Constrained Redundant GMM (CR-GMM) in the following discussion. In this experiment, the initial number of sub-components is set to 16, and the real data is sampled from QPSK modulation, i.e., 4 partially overlapped clusters. In each experiment, the convergence of likelihood as well its local enlarged curve will be shown in the upper area of the figure. Each important change points in the convergence curve will be flagged with indexes, which will be shown with constellation slices in lower figure.

As can be seen from Fig.6, for each deletion of redundant sub-components after the first three convergences, the likelihood will be re-converged to almost the same value around -1.4. However, in the deletion flagged with index 4, the deletion was triggered with only 4 sub-components left, i.e., the ground truth. As the algorithm has no idea about this, it moved forward to delete one more sub-component and resulted in a significantly decreased likelihood. Then after the re-convergence in the time flagged with index 5, the algorithm enters the process of redundant sub-component correction, and finally converged to the ground truth in index 6.

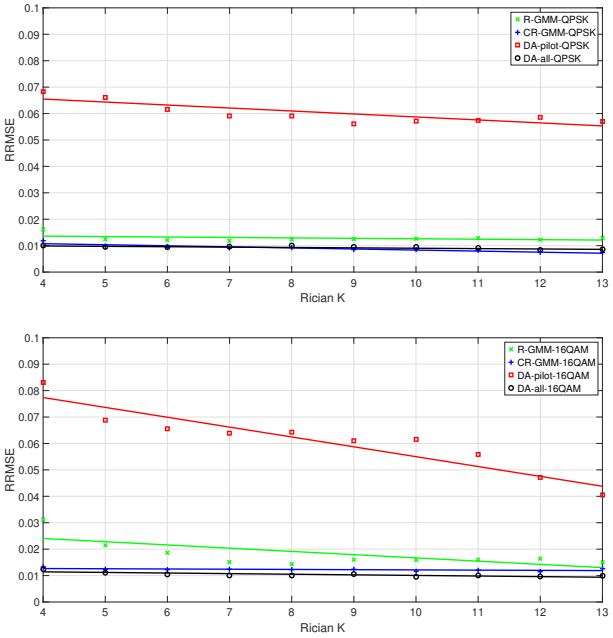

Fig. 8. RRMSE of Rician parameter estimations with different Rician K values in QPSK and 16QAM scenario.

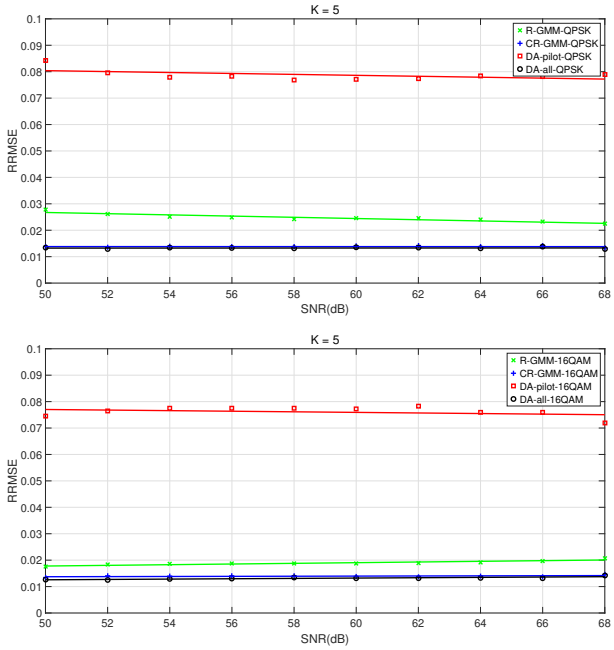

Fig. 9. RRMSE of Rician parameter estimations with different SNRs in QPSK and 16QAM scenario.

The situation will be different in Fig.7, where the constellation topology constraints have been involved. As predicted by Lemma 3, the first convergence flagged with index 1 will form a clear binary classification over likelihoods of sub-components, which is essentially different with the first crowded convergence in Fig.6. As a result, one deletion will lead to the ground truth, i.e., significantly decreased iterations.

B. Numerical Results

The performance of the proposed Rician parameter estimation algorithms is first quantitatively evaluated by intensive numerical experiments. In each numerical experiment, known Rician parameters were utilized to generate a stream of I/Q samples consisting of 127byte*8bit*16chip with various modulation order. This frame length is chosen according to the widely utilized IEEE 802.15.4 standard in industrial scenarios [28]. For the comparison purpose, the main stream Data Aided Rician parameters estimation method was also implemented, where around 3% I/Q symbols are assumed with known information, i.e., the preamble length of IEEE 802.15.4 packet. The results of this method are labelled as DA-pilot. Another candidates for comparison is the ideal DA-all mode, where all the received I/Q samples are known symbols (pilots). Obviously, the DA-all mode is an ideal situation where all symbols are utilized for channel measurement and no symbol for data transmission. As a result, the results of DA-all mode can be treated as an ideal lower bound of estimation error in this evaluation.

In Fig.8, the Relative Root Mean Square Error (RRMSE) performances of the Rician parameter estimation with both proposed non-data aided methods and classical data aided methods have presented. The results have been grouped into two groups, where all the results of QPSK have been shown in the upper sub-figure and all the results of 16QAM have been shown in the lower sub-figure. The initial constellation constraint of $\boldsymbol{A}$ and $\boldsymbol{\phi}$ have been set to 64QAM in CR-GMM, as both QPSK and 16QAM are the subsets of 64QAM. Similarly, the initial number of sub-components in R-GMM was set to 64 as well. In all scenarios, the proposed methods quickly converge to the similar performance of DA-all, i.e., the rough lower bound. As a comparison, the mainstream DA-pilot method shows almost 8 time higher error. There are slightly worse performances with small K for R-GMM, which are reasonable as the clusters in constellation will involve large overlap. This overlap not only increases the difficulty of convergence but also decreases the accuracy of estimation results. In the same time, the CR-GMM has shown constant performance in all scenarios, which is due to the involved constellation constraint.

In Fig.9, the experiment results of proposed algorithm under various SNRs have been provided to validate the effect with internal thermal noise ω. It should be noted that the internal thermal noise is usually static within short time scale, then the variation is in fact caused by the received signal strength. In this experiment, the variation scale of received signal power, i.e., from 50dBm to 68dBm, is obtained from the field experiment shown later in section C. The power of internal noise is set to -90dBm according to popular IEEE 802.15.4 transceivers utilized in industrial networks [28]. The true value of K was set to 5 as a challenging scenario. The overall performance is similar to Fig.8, where the CR-GMM approaches the optimal DA-all method around RMSE 0.012 in both QPSK and 16QAM scenarios. Although the performance shows the correlation with the increased power of internal noise, the trends are much less significant versus the Rician

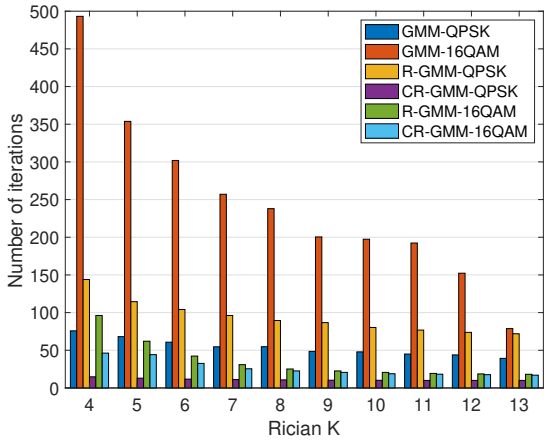

Fig. 10. Convergence performance with different Rician K values.

parameters, as shown in Fig.8.

The convergence performances of proposed methods with comparisons have been provided in Fig.10. The baseline algorithms, i.e., GMM-QPSK and GMM-16QAM, have been assumed with known information of Modulation order. With known modulation order, the GMM-QPSK converged faster than the R-GMM-QPSK in all scenarios, i.e., around 70 iterations for GMM-QPSK and around 140 iterations for R-GMM-QPSK in the harsh $K = 4$ scenario. Obviously, this is due to the additional deletion process in the R-GMM-QPSK. As expected, with the constellation constraint, CR-GMM converged much faster, say around 10 iterations. Simultaneously, an interesting phenomenon can be noticed in 16-QAM scenarios, where GMM-16QAM converged extremely slow after almost 480 iterations. This is due to the significantly increased DoFs in the EM solution with 16-QAM. However, the R-GMM-16QAM converged much faster than the GMM-16QAM with only around 90 iterations, which was not expected, especially with additional deletion processes. If further look into the converging process, the redundant sub-components (64 in the experiment) will converged to only 16 clusters in R-GMM-16QAM, while the GMM-16QAM expects 16 sub-components converged to 16 clusters. As a result, R-GMM-16QAM will always have at least one sub-component converged to each clusters, leading to an even faster converge process than GMM-16QAM with known modulation orders. Similarly, with constellation constraint, CR-GMM-16QAM will be converged around 40 iterations for $K = 4$ scenario, and only 15 iterations for $K = 13$ scenario.

C. Field Results

In this subsection, the proposed algorithm has been evaluated with field experiments in a rolling mill, which is around $300 \times 20 \times 10$ meters large, with a moving gantry crane near the roof. A logistical vehicle and several operators were asked to work around the transmission link to emulate three typical industrial working scenarios, i.e., direct link, with nearby operators, and with nearby vehicle. In the experiments, two NI USRP-2922 SDR transceiver platforms with omni-directional antennas have been deployed to form a fixed wireless link, which enable the emulation of adaptive modulation, i.e., QPSK and 16-QAM in this experiment. The threshold were shown with black lines in Fig.11. Similar as the numerical experiments, all the received I/Q streams have been recorded and processed by the chosen algorithms. For comparison, the results of DA-pilot and DA-All have been provided as well.

TABLE I
THE RRMSE OF DIFFERENT ESTIMATION METHODS

	Direct	Person	Vehicle
DA-pilot	0.0726	0.0832	0.0755
CR-GMM	0.0141	0.0161	0.0139
DA-all	0.0127	0.0143	0.0130

The estimated s and σ of each frame in the selected scenarios have been provided in Fig.11. Without any doubt, the proposed CR-GMM method shows non-sensitivity with the adaptive modulation scheme, and shows the closest performances with DA-all in all scenarios, i.e., the near optimized quantitative RRMSE results shown in Table 1. In detail, 0.0141 versus 0.0127 with direct link, 0.0161 versus 0.0143 with moving operators, and 0.0139 versus 0.013 with moving vehicle. These demonstrate the applicable of proposed method in different channel scenarios. In the same experiments, the DA-pilot algorithm show not only bias but also high jitter in all scenarios, which may lead to mis-understanding of the link quality. These field experiments further validate the efficiency of proposed method to enable its wider application.

VII. Conclusion and Future Works

In this paper, a novel non-data aided method to estimate the Rician parameters without any *a priori* information has been proposed. The problem was characterized as a GMM estimation with unknown cluster numbers, which can be solved with iterative deletion of redundant sub-components until the ground truth. To satisfy this target, the convergence paradigm with redundant sub-components based GMM has been proposed, which has been further constrained with constellation topology to increase the discrimination capability. Both numerical experiment and field experiment demonstrate the near optimal accuracy of the proposed algorithm with affordable computation cost. Although the proposed R-GMM method without constraint acceleration was intuitively to be believed as high cost with its classification and deletion loop, the over cost may even less than the standard GMM with known cluster numbers in the challenging scenarios with high DoFs. As a result, the proposed converge paradigm with redundant sub-components based GMM is also expected to be widely utilized by researchers in other scientific areas. We will also investigate the closed form solution of optimal number of sub-components in GMM, which fits in the future works.

References

[1] T. S. Rappaport and C. D. Mcgillem, "UHF Fading in Factories," *IEEE Journal on Selected Areas in Communications*, vol. 7, no. 1, pp. 40–48, 1989.

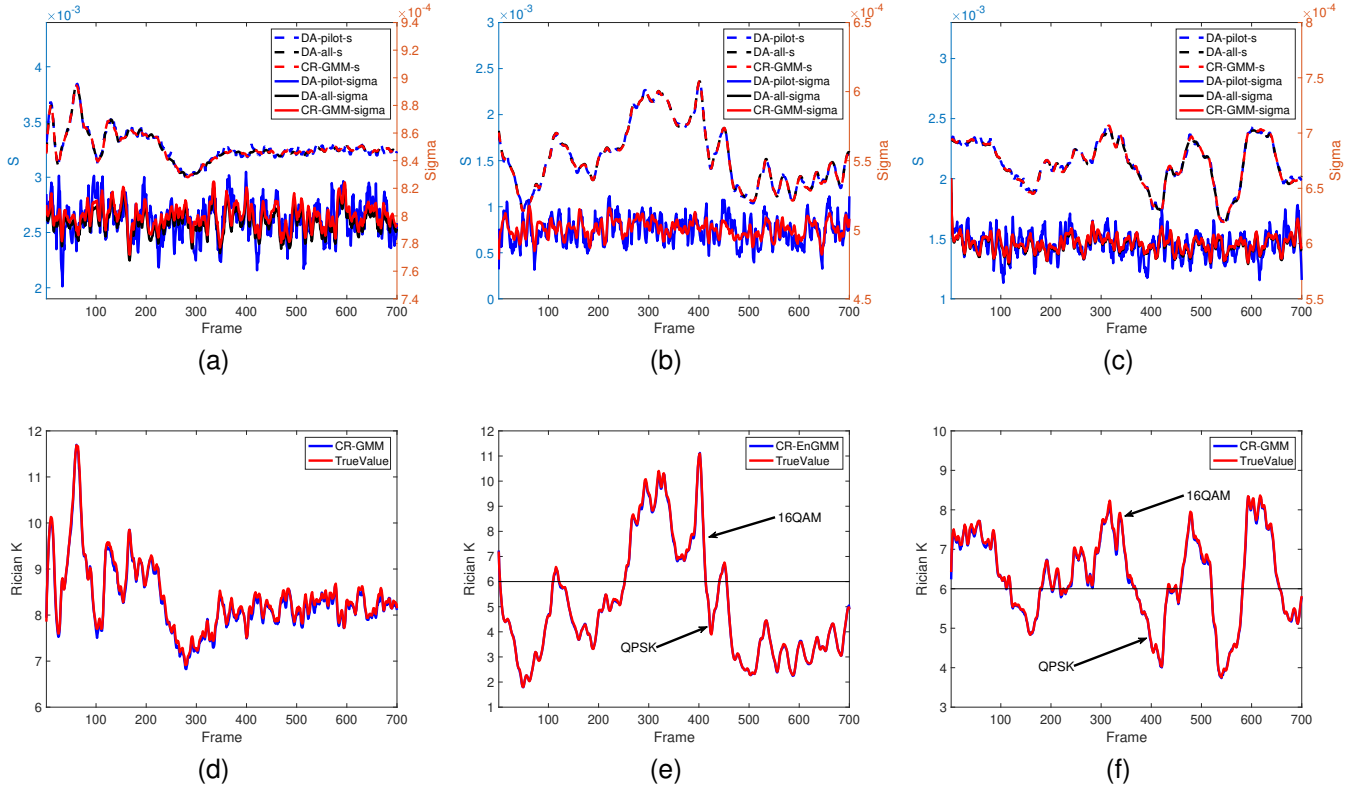

Fig. 11. Rician parameter estimations in field experiments: (a) s and σ in direct scenario, (b) s and σ with moving operators, (c) s and σ with moving vehicle, (d) K in direct scenario, (e) K with moving operators, (f) K with moving vehicle

[2] E. Tanghe, W. Joseph, L. Verloock, L. Martens, H. Capoen, K. Van Herwegen, and W. Vantomme, "The Industrial Indoor Channel: Large-scale and Temporal Fading at 900, 2400, and 5200 MHz," *IEEE Transactions on Wireless Communications*, vol. 7, no. 7, pp. 2740–2751, 2008.

[3] H. Hashemi, M. McGuire, T. Vlasschaert, and D. Tholl, "Measurements and Modeling of Temporal Variations of the Indoor Radio Propagation Channel," *IEEE Transactions on Vehicular Technology*, vol. 43, no. 3, pp. 733–737, 1994.

[4] P. Agrawal, A. Ahlen, T. Olofsson, and M. Gidlund, "Long Term Channel Characterization for Energy Efficient Transmission in Industrial Environments," *IEEE Transactions on Communications*, vol. 62, no. 8, pp. 3004–3014, 2014.

[5] M. Cheffena, "Propagation Channel Characteristics of Industrial Wireless Sensor Networks [Wireless Corner]," *IEEE Antennas and Propagation Magazine*, vol. 58, no. 1, pp. 66–73, feb 2016.

[6] M. Eriksson and T. Olofsson, "On Long-Term Statistical Dependences in Channel Gains for Fixed Wireless Links in Factories," *IEEE Transactions on Communications*, vol. 64, no. 7, pp. 3078–3091, 2016.

[7] F. Qin, Q. Zhang, W. Zhang, Y. Yang, J. Ding, and X. Dai, "Link Quality Estimation in Industrial Temporal Fading Channel with Augmented Kalman Filter," *IEEE Transactions on Industrial Informatics*, vol. 15, no. 4, pp. 1936–1946, 2019.

[8] Y. Yang, Y. Li, W. Zhang, F. Qin, P. Zhu, and C. X. Wang, "Generative-Adversarial-Network-Based Wireless Channel Modeling: Challenges and Opportunities," *IEEE Communications Magazine*, 2019.

[9] M. Luvisotto, Z. Pang, and D. Dzung, "Ultra High Performance Wireless Control for Critical Applications: Challenges and Directions," *IEEE Transactions on Industrial Informatics*, vol. 13, no. 3, pp. 1448–1459, 2017.

[10] G. P. Zhao, M. A. Imran, Z. Pang, Z. Chen, and L. Li, "Toward Real-Time Control in Future Wireless Networks: Communication-Control Co-Design," *IEEE Communications Magazine*, vol. 57, no. 2, pp. 138–144, 2019.

[11] Y. Chen and N. C. Beaulieu, "Estimation of ricean K parameter and local average SNR from noisy correlated channel samples," *IEEE Transactions on Wireless Communications*, vol. 6, no. 2, pp. 640–648, 2007.

[12] J. Wang, Y. Cui, H. Jiang, G. Pan, H. Sun, J. Li, and H. Esmaiel, "Estimation of Rice Factor Ratio for Doubly Selective Fading Channels," *IEEE Access*, 2020.

[13] I. Bousnina, M. B. B. Salah, A. Samet, and I. Dayoub, "Ricean K-factor and SNR Estimation for M-PSK Modulated Signals Using the Fourth-order Cross-moments Matrix," *IEEE Communications Letters*, vol. 16, no. 8, pp. 1236–1239, 2012.

[14] M. B. Ben Salah and A. Samet, "Moment-Based Joint Estimation of Ricean K-Factor and SNR Over Linearly-Modulated Wireless SIMO Channels," *Wireless Personal Communications*, vol. 91, no. 2, pp. 903–918, 2016.

[15] Q. Zhang, G. Lu, W. Zhang, F. Shen, X. Dai, J. Jiao, and F. Qin, "Non-Data Aided Rician Parameters Estimation in Temporal Fading Channel with 3 DoFs Gaussian Mixture Model," *IEEE Access*, vol. 7, pp. 62 198–62 209, 2019.

[16] P. Shaft, "On the Relationship Between Scintillation Index and Rician Fading," *IEEE Transactions on Communications*, vol. 22, no. 5, pp. 731–732, 1974.

[17] G. Azemi, B. Senadji, and B. Boashash, "Ricean K-factor estimation in mobile communication systems," *IEEE Communications Letters*, 2004.

[18] X. Leturc, P. Ciblat, C. J. L. Martret, P. D. Shaft, X. Leturc, P. Ciblat, and C. J. Le Martret, "Estimation of the Ricean K Factor in the Presence of Shadowing," *IEEE Transactions on Communications*, vol. 24, no. 1, pp. 108–112, 2020.

[19] C. Tepedelenlioglu, A. Abdi, and G. B. Giannakis, "The Ricean K Factor: Estimation and Performance Analysis," *IEEE Transactions on Wireless Communications*, vol. 2, no. 4, pp. 799–810, 2003.

[20] Y. Chen and N. C. Beaulieu, "Maximum Likelihood Estimation of the K Factor in Ricean Fading Channels," *IEEE Communications Letters*, vol. 9, no. 12, pp. 1040–1042, 2005.

[21] K. Baddour and T. Willink, "Improved Estimation of the Ricean K-factor from I/Q Fading Channel Samples," *IEEE Transactions on Wireless Communications*, vol. 7, no. 12, pp. 5051–5057, 2008.

[22] P. Mukherjee, D. Mishra, and S. De, "Gaussian Mixture Based Context-Aware Short-Term Characterization of Wireless Channels," *IEEE Transactions on Vehicular Technology*, 2020.

[23] B. J. Frey and D. Dueck, "Clustering by passing messages between data points," *Science*, vol. 315, no. 5814, pp. 972–976, 2007.
[24] A. Rodriguez and A. Laio, "Clustering by fast search and find of density peaks," *Science*, vol. 344, no. 6191, pp. 1492–1496, 2014.
[25] G. Stuber, *Principles of Mobile Communication*, 3rd ed. Springer, 2012.
[26] C. G. Koay and P. J. Basser, "Analytically Exact Correction Scheme for Signal Extraction from Noisy Magnitude MR Signals," *Journal of Magnetic Resonance*, vol. 179, no. 2, pp. 317–322, 2006.
[27] R. Bhattacharjea, G. D. Durgin, and C. R. Anderson, "Estimation of Rician K-factors from Block-averaged Channel Measurements," *IEEE Transactions on Wireless Communications*, vol. 11, no. 12, pp. 4231–4236, 2012.
[28] Texas Instruments, "CC2420 Datasheet," 2008. [Online]. Available: https://www.ti.com/lit/ds/symlink/cc2420.pdf